20. Requena, J. M., Jimenez-Ruiz, A., Soto, M., Assiego, R., Santaren, J. F., Lopez, M. C., Patarroyo, M. E. & Alonso, C. 1992. Regulation of hsp70 expression in *Trypanosoma cruzi* by temperature and growth phase. *Mol. Biochem. Parasitol.*, **53**:201–212.

21. Requena, J. M., Lopez, M. C., Jimenez-Ruiz, A., Morales, G. & Alons, C. 1989. Complete nucleotide sequence of the hsp70 gene of *T. cruzi*. *Nucl. Acids Res.*, **17**:797.

22. Requena, J. M., Lopez, M. C., Jimenez-Ruiz, A., Torre, J. C. de la & Alonso, C. 1988. A head-to-tail tandem organization of hsp70 genes in *Trypanosoma cruzi*. *Nucl. Acids Res.*, **16**:1393–1406.

23. Ritter, D. M. & Rowland, E. C. 1984. Corpus Christi strain-induced protection to *Trypanosoma cruzi* infection in C3H (He) mice: effective dose, time, route, and number of vaccinations. *J. Parasitol.*, **70**:755–759.

24. Rosfjord, E. C., Mikhail, K. S., Rowland, E. C. & Powell, M. R. 1990. Analysis of antibody cross-reactivity in experimental American trypanosomiasis. *J. Parasitol.*, **76**:698–702.

25. Rowland, E. C. & Ritter, D. M. 1984. Corpus Christi strain-induced protection to *Trypanosoma cruzi* infection in C3H (He) mice: transfer of resistance to Brazil strain challenge with lymphocytes. *J. Parasitol.*, **70**:760–766.

26. Sambrook, J., Fritsch, E. F. & Maniatis, T. 1989. Molecular Cloning. A Laboratory Manual, 2nd ed. Cold Spring Harbor Laboratory Press, Cold Spring Harbor, New York.

27. Sanger, F., Nicklen, S. & Coulson, A. R. 1977. DNA sequencing with chain-terminating inhibitors. *Proc. Natl. Acad. Sci.* (USA), **74**: 5463–5467.

28. Wallace, G. R., Ball, A. E., MacFarlane, J., Safi, S. H. el, Miles, M. A. & Kelly, J. M. 1992. Mapping of a visceral leishmaniasis-specific immunodominant B-cell epitope of *Leishmania donovani* Hsp70. *Infect. Immun.*, **60**:2688–2693.

29. Watowich, S. S. & Morimoto, R. I. 1988. Complex regulation of heat shock- and glucose-responsive genes in human cells. *Mol. Cell. Biol.*, **8**:393–405.

Received 5-27-93, 12-8-93; accepted 3-7-94

J. Euk. Microbiol., 41(5), 1994, pp. 441–450

A Morphometric Analysis of the *Euplotes charon* Morphotype (Ciliophora: Euplotida)

THOMAS C. JONES and MICHAEL A. GATES[1]

Department of Biology, Cleveland State University, Cleveland, Ohio 44115

ABSTRACT. Twenty-one different strains of *Euplotes* of the cirrotype 10, double dargyrome morphotype were collected in marine and brackish habitats from widely varying geographic locations. The strains were cultured under similar conditions prior to fixation and staining. The morphological features considered included the cell lengths and widths, the number and position of all the ventral cirri, adoral membranelles and dorsal cilia, and the position of the peristomal shelf. Univariate and multivariate analyses revealed continua in these measurements among the strains, as well as significant correlations between cell length and the number of adoral membranelles, the number of dorsal cilia, and the length, width and area of the oral cavity. Based on data from this study and from previous studies, we conclude that the traditional criteria used for species descriptions within this morphotype are insufficient to provide robust distinctions. Therefore, we submerge all of the descriptions within this morphotype under the nomenclaturally superior *Euplotes charon* Müller, 1786.

Supplementary key words. Euplotidae, hypotrichs, principal components analysis, species problem, systematics.

ONE of the goals of taxonomy is to describe the limits of observable variation in nature by superimposing hierarchical levels of classification upon living organisms, in the hope that the resulting order will consistently reflect evolutionary relationships among them. As molecular phylogenies for protists are not common, the taxonomic divisions at all hierarchical levels of this group are mostly based on morphological descriptions [9, 41]. More robust methods of ascertaining evolutionary relationships within genera which exhibit asexuality involve molecular techniques in constructing phylogenies (e.g. rRNA sequencing and DNA hybridization). Despite the directness of these techniques, such studies need to examine numerous strains, preferably from widespread locations, to be confident that any significant differences observed are not simply local extremes of a continuum of genetic variability.

The taxonomy of the ciliate genus *Euplotes* is controversial, with no consistent guidelines for defining the boundaries of species [6, 11, 16, 18, 19, 29–35, 47, 51, 52]. Assigning species within *Euplotes*, and within genera containing asexual strains, is problematic in that reproductive isolation cannot always be used as a diagnostic criterion. General morphological descriptions have been the basis of the vast majority of species descriptions within this and other ciliate genera. There exist, in the literature for the genus *Euplotes*, several remarkably similar descriptions of supposedly different species; but there have been very few attempts to quantify the morphological observations in these descriptions beyond such gross measures as cell length and/or width [6, 7, 11, 32, 35, 47].

As long as morphology is to be used as a mainstay of taxonomy, the analysis of tentative differentiating traits should be performed in such a way that the conclusions drawn are robust. This is particularly true in ciliate taxonomy, where differences among strains are often subtle, and traits frequently form continua among strains. Therefore, morphological descriptions need to be quantitative and statistical in order to avoid subjectivity and bias, and they should focus on the observed limits of variation of the considered traits, rather than just the central tendencies [16]. Furthermore, bias can arise, even in quantitative analysis, in choosing only a few characters to examine. Such trait-dependent biases are lessened through multivariate analysis, in which several attributes are examined simultaneously. Examples of the power of multivariate ciliate morphometrics are studies of morphological stability over time [22, 23] and of growth cycle changes [45] in the *Tetrahymena pyriformis* complex, of syngenic ascertainment in the *Paramecium aurelia* complex of sibling species [24, 27, 38], and of ventral cirral patterns [15, 17, 18, 51], dorsal ciliary patterns [20], and population differentiation [21] in *Euplotes* populations.

[1] To whom correspondence should be addressed.

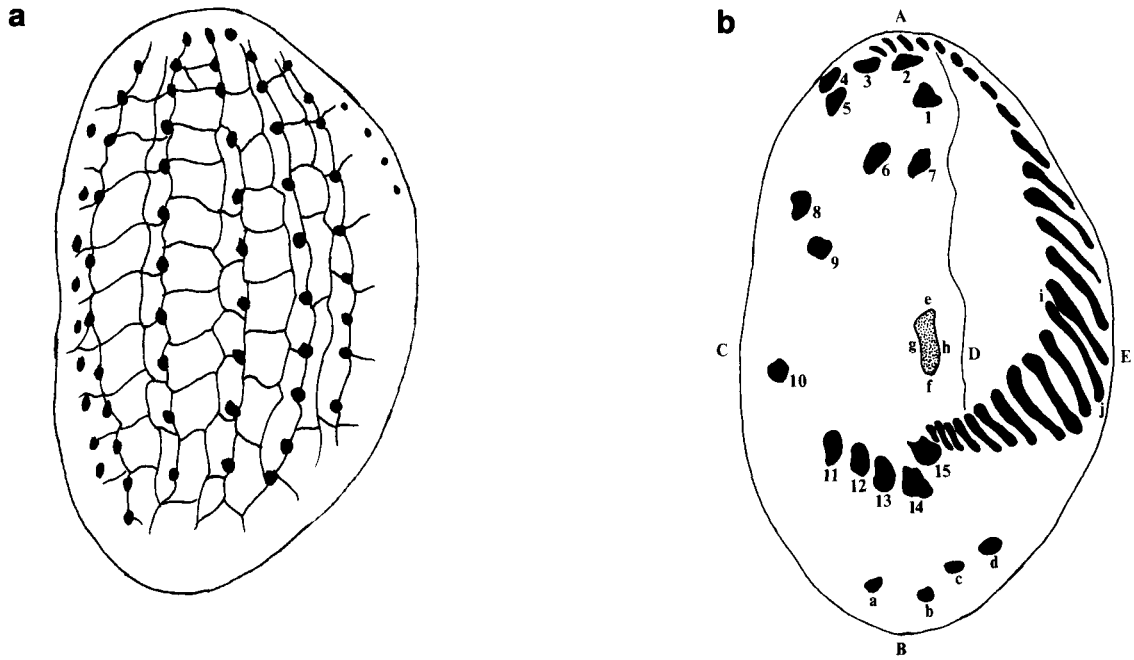

Fig 1. Diagrams of ventral and dorsal surfaces of an *E. charon* morphotype *Euplotes*. **a**. Diagram of the dorsal surface of a double dargyrome *Euplotes*. **b**. Diagram of the ventral surface of a cirrotype 10 *Euplotes* with the digitized points identified. Figure abbreviations: A, anterior cell margin; B, posterior cell margin; C, right cell margin; D, point where the peristomal shelf crosses the width axis; E, left cell margin; 1–10, frontoventral cirri; 11–15, transverse cirri; a–d, caudal cirri; e–h, anterior, posterior, right and left (respectively) margins of the paroral membranelle; i & j, endpoints of the longest adoral membranelle.

Euplotes provides an convenient model system for morphometric analyses of ciliates. Clonal populations isolated from natural samples may be objectively classified on the basis of two general but stable taxonomic features [16, 19]: the cirrotype and the dargyrome. The cirrotype [18] is the total number of frontoventral cirri on the ventral surface (see Fig. 1b), which ranges from 7–10. The dargyrome [25] is the dorsal argentophilic network, corresponding to subpellicular vacuolar boundaries (see Fig. 1a), and observed patterns may be categorized as either single, double, or multiple [11, 25].

One of the most commonly collected types of *Euplotes* found in marine shoreline samples has frontoventral cirrotype 10 and a double dargyrome (pers. observ. over many years). Strains of this morphotype, referred to as the *charon* morphotype [19], are commonly small (about 40–60 μm in length) and fit the general description of several classical "species" in the taxonomic literature: the marine species *E. alatus* [6, 32], *E. antarcticus* [13], *E. balteatus* [4, 32, 47, 48], *E. charon* [2, 5, 10, 11, 32, 47, 50], *E. harpa* [18, 47], *E. magnicirratus* [7], *E. neapolitanus* [54], *E. octocirratus* [1], *E. polycarinatus* [7], *E. quinquecarinatus* [6, 28], *E. rariseta* [12], *E. trisulcatus* [5, 7, 32, 47], and *E. tuffraui* [4], and the freshwater species *E. crenosus* [47], *E. inkystans* [47], and *E. palustris* [46].

We have obtained and cultured numerous strains of this cirrotype 10, double dargyrome morphotype from widespread geographic locations; small cells of this *charon* morphotype are in fact the most common *Euplotes* found in our marine samples. Using quantitative methods, we will describe the extent of morphological variation within and among populations belonging to this general morphotype and relate it to the existing taxonomy.

MATERIALS AND METHODS

Cultivation. *Euplotes* from raw samples (collected from various geographic locations described in Table 1) were isolated as single cells along with native bacteria. These clonal cultures were maintained in polystyrene culture tubes in an artificial seawater medium supplemented with soil and cereal grass extracts [details given in 18, 26]. Culture tubes were kept at ambient temperature (22–26° C) with an irregular light cycle, but with at least eight hours of darkness each night. Every two weeks half of the medium was poured off and replaced with fresh medium.

Identification. No attempt was made a priori to assign clonal strains to particular nominal species on the basis of published typological descriptions. Silver-stained specimens of all strains initially were examined only to verify the general *charon* morphotype [19]. Strains used for this study initially were chosen as "small" cirrotype 10, double-dargyrome *Euplotes*, with the exception of strain Kli2, a "medium" *charon*-morphotype *Euplotes* that was included for comparison with the "small" strains.

Morphometric data collection. Cell cultures were concentrated by centifugation before fixation and staining with a modified Chatton-Lwoff protocol [8, 14]. Cell measurements were taken using a Leitz Dialux microscope equipped with bright field planapochromatic optics and a Leitz tracing device (Ernst Leitz Wetzlar GMBH, Wetzlar, Germany). Specimens were viewed at 500× magnification for simple length/width measurements, and at 1,250× under oil immersion for more detailed measurements. All specimens selected for measurement were well impregnated with silver stain, were in interphase, and had either their dorsal or their ventral surfaces oriented perpendicular to the focal axis. Cells to be measured were centered in the field of view, and the crosshairs of a Bitpad One electronic digitizer (Summagraphics, Fairfield, CT), as seen through the drawing tube, were superimposed on the various points of interest and these points digitized. Coordinate data were stored as magnetic files on a microcomputer, where they were processed using C language data manipulation programs (written by M. Gates).

For each strain, detailed measurements (Fig. 1b, Table 2) were

Table 1. List of strain designations, sampling locations and dates, sampling habitats, and one letter strain codes.

Strain	Location	Date	Habitat	Code
Acad	Bass Harbor, ME	8/88	Marine	A
Ant3	Antigua, W.I.	7/88	Marine	B
Ava3	Avalon, NJ	8/84	Marine	C
Cal4	San Simeon, CA	4/84	Brackish[a]	D
Can3	Cancun, Mexico	3/84	Marine	E
Can4	Cancun, Mexico	3/84	Marine	F
Cay2	Grand Cayman, W.I.	11/81	Marine	G
CC31	Plymouth, MA	3/90	Marine[a]	H
Del1	Dewey Beach, DL	7/87	Marine	I
Del4	Bethany Beach, DL	7/87	Marine	J
Galv1	Galveston, TX	9/82	Brackish	K
Jam6	Jamaica, W.I.	2/84	Marine[a]	L
Jfla5	Fort Lauderdale, FL	7/87	Marine[a]	M
KK8	Knights Key, FL	3/90	Marine[a]	N
Kli2	Emerald Island, NC	3/90	Marine[a]	O
Kli3	Emerald Island, NC	3/90	Marine	P
Mia1	Miami Beach, FL	7/86	Marine	Q
SI1	Chatham, MA	8/90	Marine	R
SI2	Chatham, MA	8/90	Marine	S
SI4	Chatham, MA	8/90	Marine	T
Stv2	St. Vincent, W.I.	12/88	Marine	U

[a] Encystment was observed in this strain.

Table 2. List and description of linear measurements and counts for the ventral surface of cirrotype 10 *Euplotes*; standard points refer to landmarks on Fig. 1b.

Trait	Point	Point	Description
1	A	B	Cell length
2	C	E	Cell width
3	C	D	Ventral plate width
4	2	7	Streak I, top section
5	7	15	Streak I, bottom section
6	3	6	Streak II, top section
7	6	14	Streak II, bottom section
8	4	5	Streak III, top section
9	5	13	Streak III, bottom section
10	8	9	Streak IV, top section
11	9	12	Streak IV, bottom section
12	10	11	Streak V
13	1	15	Buccal cirrus-transverse cirrus 1
14	2	14	Frontoventral-transverse (FVT) field
15	7	8	Width of FVT field
16	7	10	Oblique mid-width of FVT field
17	4	7	Oblique anterior FVT field width
18	11	15	Width of transverse cirral (TC) field
19	11	14	Lateral length of TC field
20	—	—	Number of caudal cirri
21	—	—	Mean spacing of caudal cirri
22	—	—	# of adoral zone membranelles (AZM)
23	—	—	Mean spacing of AZM
24	i	j	Maximum width of AZM
25	e	f	Paroral membranelle (PM) length
26	g	h	PM width
27	A	14	Anterior cell margin to TC
28	A	e	Anterior cell margin to PM top
29	C	g	Right cell margin to right PM margin

taken of 25 ventral surfaces, including the endpoints of the length and width axes (and the point where the peristomal shelf crosses the width axis), the positions of the individual frontoventral, transverse and caudal cirri, the positions of the inner edges of the adoral zone of membranelles and the endpoints of the paroral membrane (along the length and width axes). Measurements of 25 dorsal specimens (necessarily different specimens from the ventral measurements) included the number and position of the kineties, and the number and position of the kinetosomes within each kinety. Also on the dorsal surface, the central point of each sub-pellicular vacuole in the central three rows (the right-most row being determined by the anterior end of the AZM) was digitized.

Statistical methods. The general univariate statistics used (means, variances, etc.) are described in Sokal & Rohlf [42]. The sums of squares simultaneous test procedure (SSSTP) analyses were done on an 80386-based microcomputer, using the program given in Sokal & Rohlf [42]. This method tests all possible comparisons among means and identifies groups of means which are significantly different from one another. The standard 95% confidence level was used throughout this study.

All other statistical analyses were performed with the S package of interactive programs [3] on a minicomputer. Boxplots (box-and-whisker plots [49]) were used to graphically present some data because they give a clear picture of both the central tendencies and the spread of the data. The "box" of the boxplot encapsulates the central 50% of the data (defined by the upper and lower quartiles), with the centerline denoting the median. The "whiskers" encompass the standard range of the data, with very extreme values plotted as asterisks.

Multivariate analysis was conducted using principal components analysis (PCA) [36, 44], which produces an orthogonal rotation of the data in their original multidimensional space, such that the greatest variation in the data lies along the first principal component axis, the second greatest variation lies along the second principal component axis, and so on.

In this study PCA was done in two different ways. One way was by taking all the variables (including the counts) and scaling them. This procedure uses the correlation matrix, so that the variances of all the scaled variables were 1.0, and the mean of each variable was 0.0. This method must be used when including the counts in the data. The other method excluded the counts from the data, thereby creating a matrix in which all of the units were the same (micrometers). This method employs the covariance matrix, and gives a truer sense of the variational structure of linear data [44].

Cirral patterns were analyzed using the frequency distribution of relative intercirral distances [15] and were compared using the Kolmogorov-Smirnov statistic (K-S statistic [42]).

RESULTS

Univariate analyses. The mean cell lengths among the strains ranged from 36.90 μm (Jfla5) to 77.13 μm (Kli2). By the SSSTP test and by boxplot analysis, the majority of the strains formed an overlapping group of means (Table 3, Fig. 2a), while strain Kli2 was significantly larger than all the others, and strains Ava3 and Del4 formed an intermediate group of overlapping means.

The mean cell widths ranged from 26.68 μm (Acad) to 55.34 μm (Kli2). The majority of the strains formed a large overlapping group, consisting of the same strains that made up the most numerous group with respect to mean lengths (Table 3, Fig. 2b). Strains Ava3, Del4 and Kli2 (in order of increasing cell widths) were each significantly different from all the other strains.

Univariate analyses of the detailed ventral measurements by SSSTP revealed various degrees of overlap among the strain means (Table 3). For several measurements there was complete overlap among the 21 strains. Overall, however, strain Kli2 tended to be significantly larger than all of the other strains, followed by the strains Ava3 and Del4, which were often significantly larger than the other strains but often not from each

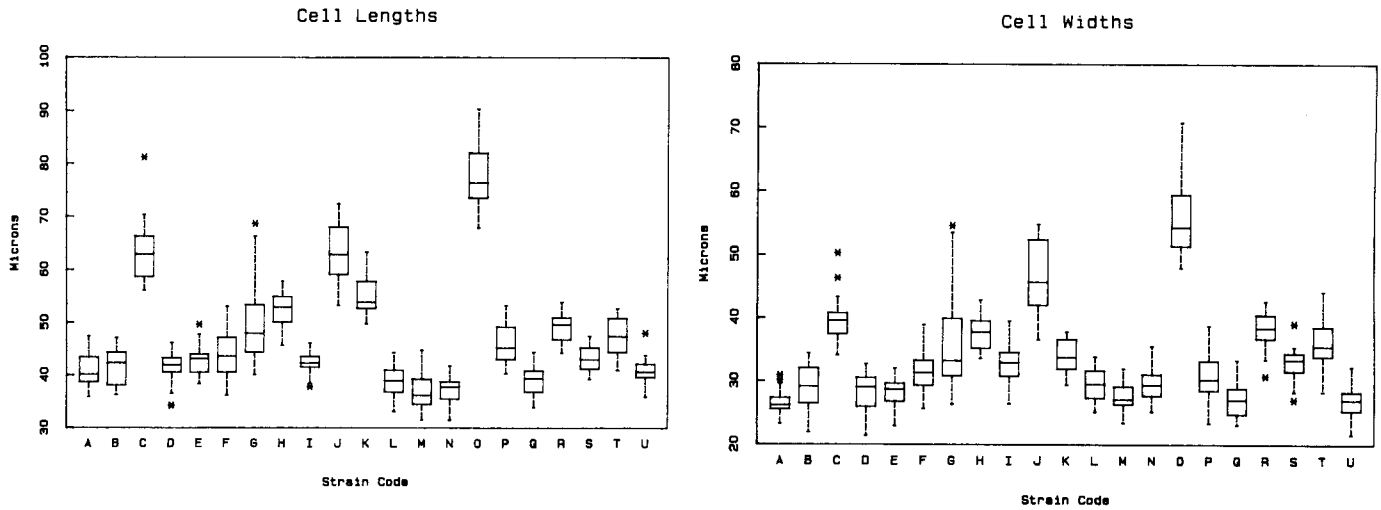

Fig. 2. Boxplots of cell lengths and widths of *E. charon* morphotype strains. The strain codes (A–U) are given in Table 1; C, J and O are strains Ava3, Del4 and Kli2, respectively. **a**. Boxplots of cell lengths. **b**. Boxplots of cell widths.

other. Strain KK8 was significantly smaller than all the other strains for several measurements, including four intercirral streak measurements and the number of membranelles in the AZM (Table 3). The number of adoral membranelles was highly and significantly correlated with overall cell length (the product-moment correlation coefficient, $r = 0.85$ [$P < 0.014$]). Cell length also was highly and significantly correlated with the length of the oral cavity (measurement 28: $r = 0.89$ [$P < 0.01$]), the width of the oral cavity (measurement 2 − measurement 29: $r = 0.79$ [$P < 0.01$]), and an estimate of the area of the oral cavity (½ the length times the width: $r = 0.88$ [$P < 0.01$]).

SSSTP analyses for the dorsal measurements revealed that strain Kli2 had significantly more kinetosomes overall and in the central kinety. For these two dorsal counts, the other strains formed several overlapping groups, different from those for the ventral measurements (Table 3). Mean kinetotype also had a

Table 3. Results of the sums-of-squares simultaneous test procedure (SSSTP). Groups of strains not significantly different in their mean values are enclosed in brackets.

Measurement	Non-overlapping groups
1	[A, B, D–I, K–N, P–U] [C, J] [O]
2	[A, B, D–I, K–N, P–U] [C] [J] [O]
3	[A–U]
4	[A–U]
5	[N] [A, B, D–G, I, K–M, P–U] [C, H, J, O]
6	[A–J, L–U] [K]
7	[N] [A–M, P–U] [O]
8	[A–U]
9	[N] [A–M, P–U] [O]
10	[A, C–U] [B]
11	[A, B, D–G, I, L–N, P–U] [C, H, J, K, O]
12	[A–U]
13	[A, B, D–N, P–U] [C] [O]
14	[N] [A, B, D–I, K–M, P–U] [C] [O]
15	[A–I, K–N, P–U] [J, O]
16	[A–I, K–N, P–U] [J, O]
17	[A–U]
18	[A–N, P–U] [O]
19	[A, B, D–F, H, I, K–N, P–U] [C, G, J, O]
20	[A–U]
21	[A–U]
22	[N] [A–M, P–U] [O]
23	[A] [B–U]
24	[A–N, P–U] [O]
25	[A–N, P–U] [O]
26	[A–U]
27	[A, B, D–I, K–N, P–U] [C, J] [O]
28	[A, B, D–I, L–N, P–U] [C, J, K] [O]
29	[A–I, K–N, P–U] [J, O]
# Central kinetosomes	[A–J, L–N, P–U] [K] [O]
# Kinetosomes total	[A, B, E, F, I, N, Q–U] [C, D, L, G, H, J, K, M, P] [O]

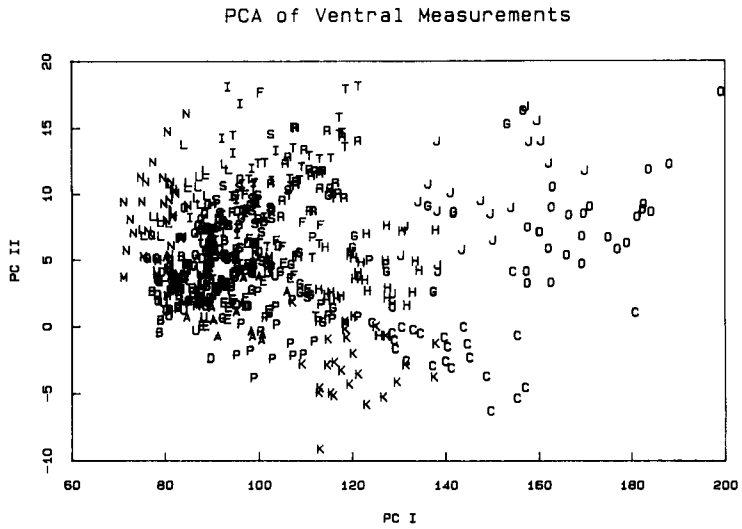

Fig. 3. Projections onto the first three principal components axes of the linear ventral measurement data of strains of *E. charon* morphotype *Euplotes*. C, J, K, and O are strains Ant3, Ava3, Del4, Galv1, and Kli2, respectively. Note that strains B (Ant3) and K (Galv1) form nearly distinct clusters in the higher values of PC II.

highly significant positive correlation with mean cell length ($r = 0.72$ [$P < 0.01$]).

Multivariate analyses. Principal components analysis of the 27 linear ventral measurements revealed considerable overlap among the 21 strains when the data were projected onto the first few principal components (PC). In this (Fig. 3) and all subsequent PCA results, only the first two components are shown, because these account for most of the variation in the data and because no additional taxonomic information was revealed by inspection of higher dimensional plots (unless otherwise indicated). However, several strains, including Ava3, Del4, and Kli2, tended to separate toward the higher values of PC I (Fig. 3). This component (which accounted for 42.8% of the total variation: loadings table not shown) correlated most highly with cell length ($r = 0.428$), measurement 27 (anterior cell margin to the transverse cirri; $r = 0.356$), measurement 14 (the length of the frontoventral-transverse (FVT) cirral field; $r = 0.337$), measurement 13 (buccal cirrus to transverse cirrus 1; $r = 0.306$) and with cell width ($r = 0.291$). All of these measurements, except cell width, are longitudinal and correlated highly with each other (data not shown). Strain KK8, which was significantly smaller than the other strains in several of the ventral measurements, was concentrated along the lower edge of the data cloud along PC I (Fig. 3). Strain Ava3 separated from strains Del4 and Galv1, but not strain Kli2, along PC II. This component accounted for 8.4% of the total variation and mainly involved a contrast between width-related measurements (2, cell width, $r = 0.578$; 29, right cell margin to the right paroral membranelle (PM) margin, $r = 0.466$), and two longitudinal measurements of the FVT cirral field (14, length of FVT field, $r = -0.215$; 28, the anterior cell margin to the anterior margin of the PM, $r = -0.240$). None of the strains separated notably along PC III, which accounted for 5.8% of the total variation (data not shown). Another linear measurement PCA was performed excluding the largest strain, Kli2, resulting in no notable changes in groupings among the remaining strains (data not shown).

A scaled PCA was performed in which all 29 of the ventral measurements (including the counts of the caudal cirri and AZM membranelles) were included. As was the case in the linear measurement PCA, strains Ava3, Del 4, and Kli2 tended to separate along the higher values of PC I (Fig. 4). Principal component I loaded most heavily on longitudinal measurements 27 (anterior cell margin to the transverse cirri, $r = 0.223$), 13 (buccal cirrus to transverse cirrus 1, $r = 0.222$), 14 (length of the FVT cirral field, $r = 0.222$), 9 (the bottom section of primordial streak 3, $r = 0.220$) and cell length ($r = 0.222$). All specimens of strains Ant3 and Galv plotted as tight clusters, almost completely isolated from the other strains in the higher values of PC II; these strains are distinct from each other along PC I (Fig. 4). Principal component II contrasted measurements 4 and 6 (the top sections of streaks I and II; $r = 0.329$ and $r = 0.451$, respectively), plus measurement 20 (number of caudal cirri, $r = 0.420$) with measurements 21 (the mean spacing of the caudal cirri, $r = -0.413$) and 16 (the oblique mid-width of the FVT cirral field, $r = -0.289$). None of the strains separated along PC III (data not shown).

A PCA of only those ventral measurements involving intercirral distances (measurements 4–19: Table 2), scaled by the overall length of the cell, also was performed. The strains overlapped considerably on the first three PC, which accounted for 20.4, 14.7 and 12.9% of the total variation, respectively. Specimens of strain KK8 were grouped towards the low end, while specimens of strain CC31 were located towards the high end of PC I (Fig. 5), which loaded most heavily on longitudinal measurements 13 (buccal cirrus to transverse cirrus 1, $r = 0.463$), 14 (the length of the FVT cirral field, $r = 0.422$), 5 (the bottom section of streak I, $r = 0.410$), 7 (the top section of streak II, $r = 0.373$) and 11 (the length of streak V, $r = 0.361$), contrasted with measurement 10 (the top section of streak IV, $r = -0.161$). Strain Galv1 specimens were clustered at the lower values of PC II (Fig. 5), which contrasted transverse measurements 15 (the width of the FVT cirral field, $r = 0.526$), 16 (oblique mid-width of the FVT cirral field, $r = 0.514$), 18 (width of the transverse cirral field, $r = 0.415$), 17 (anterior frontoventral cirral width, $r = 0.324$) and 19 (the lateral length of the transverse cirral field, $r = 0.239$) with longitudinal measurements 7 (the bottom section of streak II, $r = -0.104$), 11 (the bottom section of streak IV, $r = -0.183$), 12 (the length of streak V, $r = -0.169$)

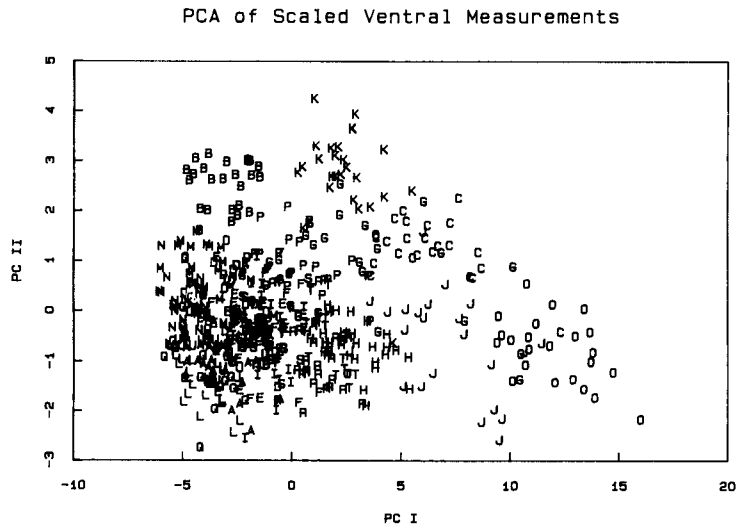

Fig 4. Projections onto the first two principle component axes of the scaled ventral measurement data for strains of *charon*-morphotype *Euplotes*. B, C, J, K, and O are strains Ant3, Ava3, Del4, Galv1, and Kli2, respectively. Note that strains Ant3 and Galv1 form nearly distinct clusters in the higher values of PC II.

and 14 (the length of the FVT field, $r = -0.140$). Both strains Galv1 and Ant3 were clustered towards the higher values of PC III (data not shown), while they separated from each other along PC II. One of the variables most important in causing this separation was measurement 11 (the bottom section of streak IV), for which strain Ant3 was noticeably smaller by boxplot analysis (having the lowest median and interquartile range of the strains: data not shown) and which highly negatively correlates with PC II ($r = -0.183$). Another important measurement involved in this separation was measurement 6 (the top section of streak II), for which strain Galv1 was noticeably larger than other strains by boxplot analysis (having an interquartile range distinctly above all other strains: data not shown) and which highly positively correlates with PC III ($r = 0.342$). Principal component III primarily contrasted measurements 4 (top section of streak I, $r = 0.494$), 6 (the top section of streak II, $r = 0.342$), 14 (the length of the FVT field, $r = 0.245$) and 17 (oblique anterior width of FVT field width, $r = 0.351$), with measurements 5 (the bottom section of streak I, $r = -0.217$), 11 (the bottom section of streak IV, $r = -0.295$) and 16 (the oblique mid-width of the FVT field, $r = -0.385$). In strain Ant3 the position of cirrus IV/2 appears to be located more posteriorly with respect to the rest of the cirri than in the other strains.

Cirral patterns. The distributions of the relative intercirral distances were calculated for each of the 21 strains. The graphical depiction of these distributions (Fig. 6) is generally bimodal, with the scatter among the strains remaining fairly constant over the majority of the relative distances. Pairwise K-S statistics were calculated for the cumulative distributions between each of the strains (data not shown); these ranged from 0.0141 (be-

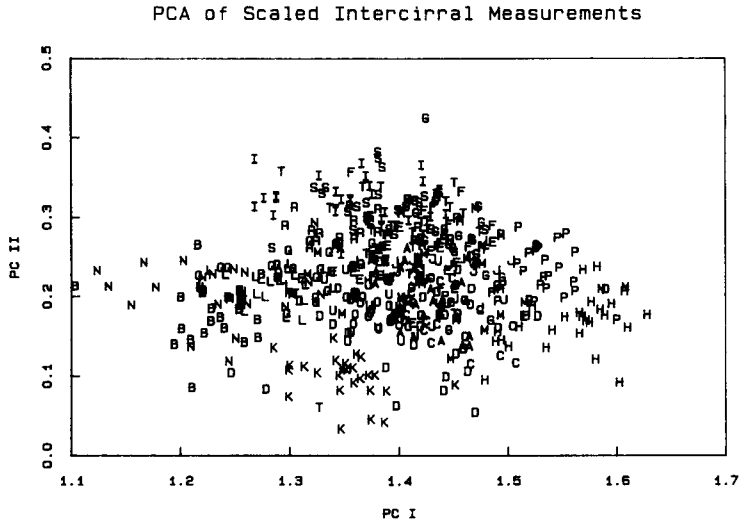

Fig. 5. Projections onto the first two principal component axes of the scaled (by cell length) intercirral measurements (4–19: described in Table 2) for strains of *charon*-morphotype *Euplotes*.B, H, K, and N are strains Ant3, CC31, Galv1, and KK8, respectively.

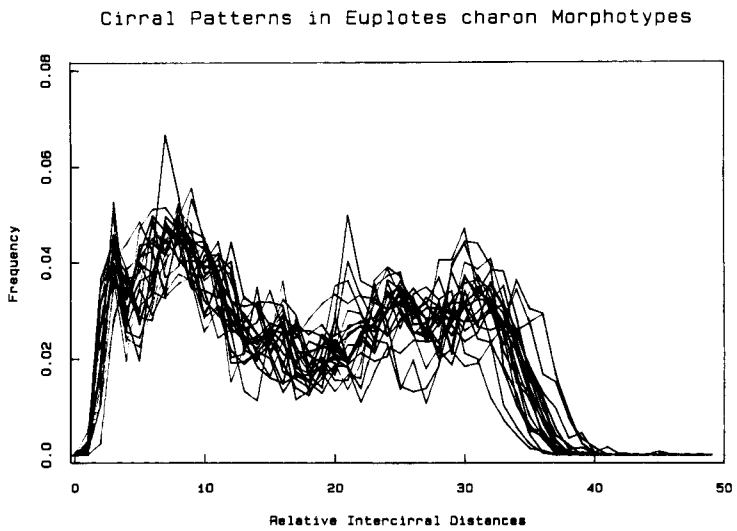

Fig. 6. Relative intercirral distance distributions for strains of *charon*-morphotype *Euplotes*.

tween strains SI2 and SI4) to 0.1728 (between strains CC31 and KK8). Using the criterion value of inherent intraclonal variability (0.0693) as a standard for assessing the significance of differences among cirral distributions [15, 18], none of the strains were different from all others, nor were any similar to all others, in cirral pattern. However, strain KK8 was significantly different from all but two other strains (Del1 and Galv1). Four of the strains (Ava3, Can3, Jfla5 and SI4) were only significantly different from three other strains, and none of these were different from each other. Strains SI1, SI2 and SI4 were collected at the same time from the same shore (Table 1), and conjugation was observed when these strains were starved and mixed (data not shown); these strains were not different from each other in cirral pattern (maximum K-S value = 0.0245). Strain Kli2, which was significantly different from all other strains in overall size, was different from only five other strains in this measure of cirral pattern.

DISCUSSION

Overall, there is considerable variation in morphological structure among strains of cirrotype 10, double dargyrome *Euplotes*. The difficulty in establishing the systematic implications of such variation lies in deciding to which variables to assign importance. Strains can significantly differ in some attributes, while being similar in others (Table 3). Overall cell size has often been used as a major differentiator among species descriptions [6, 7, 11, 32], but it has been shown elsewhere and here to be one of the most highly variable factors, within strains and particularly among strains of the *E. charon* morphotype. The great advantage of PCA is that it provides a simultaneous look at the entire variational structure of numerous measurements from many strains, and it determines, without bias, the relative importance of the variables in contributing to variation among strains. The procedure identifies each single variable, or combination of variables, that might contribute significantly to strain differences. The conclusions drawn from the results of this study will rely heavily on the robustness of PCA [36, 44].

As expected, Strain Kli2 (our subjectively assessed "medium"-sized strain) consistently separated from the other strains in overall size, in the majority of ventral measurements, and in dorsal ciliature (Table 3). In cell length and width, however, it overlapped in range with strains Ava3, Cay2 and Del1. It does not differ from the majority of strains in cirral pattern, thus supporting the assertion that cirral pattern is a highly conserved feature [16]. This strain fits fairly well the description of the classic species *E. charon* [2, 5, 10, 11, 32, 47, 50], with the exception of the dorsal ciliature, which Tuffrau [47] described as having 35–40 cilia in the central rows, which Borror [5] redescribed as being only 18–21, and which Valbonesi et al. [50] claim is "normally" 16. Our strain Kli2 averaged 13.9 cilia in the central row, with a maximum of only 17. We, however, think it imprudent to base a redescription of *E. charon* on this strain because it has been observed, in this study and in others [20, 25], that kinetotype is highly variable and scales with cell size.

The strains studied, particularly with strain Kli2 excluded, formed a continuum in cell size, ranging in mean length from 36.9 μm to 63.6 μm in strains Jfla5 and Del4, respectively. These two strains were considerably different from each other when viewed separately, in that their ranges of length and width did not overlap; they were, however, continuously "connected" by the ranges of the lengths and widths of the other strains in this study (Table 3, Fig. 2).

Considering all the ventral data simultaneously using PCA also revealed continuous variation among the strains along the different PC. Again, individual strains sometimes formed clusters distinct from certain others, but these are all bridged by other strains. Two strains (Ant3 and Galv1) form nearly distinct clusters in the first two PC based on scaled ventral measurements (Fig. 4). These separations, in each case, were mainly due to single variables involving cirral positioning.

Many of the K-S statistics comparing the cirral patterns between strains were larger than the standard criterion value for inherent clonal variability [15, 18], which was based on a subclonal analysis of a single strain of classical *E. harpa*. Three of the strains (CC31, Jam6 and KK8) exceeded this value in the majority of their comparisons, and strains CC31 and Jam6 had the highest overall K-S statistic. The PCA of only intercirral distances (Fig. 5) revealed, however, that the set of all strains formed a continuum. Strains CC31 and Jam6 are widely separated along PC I (hence their high K-S value), but they are merely the extremes of one large cluster. This set of cirrotype 10, double dargyrome strains, therefore, cannot be differentiated by their cirral patterns because none are distinct.

There was wide variation among strains with respect to measures of other ciliary structures, including the AZM number and the number of dorsal cilia. Both features showed overlap among most of the strains, although strain Kli2 was significantly higher in all three measures and strain KK8 had significantly fewer adoral membranelles (Table 3).

Ciliary beating is affected by the hydrostatic forces created by the beating of neighboring cilia, setting up metachronal waves [40]. Since the currents created by the adoral ciliary membranelles are vital to the cell's feeding, one would expect there to be strong selective pressure to maintain a functionally constrained distance between membranelles. Therefore, if the oral cavity of the cell scales with overall cell size, as in this study and in Tuffrau's [48], larger cells will most likely maintain higher numbers of adoral membranelles. This is what we have observed in our strains and what Tuffrau [48] observed within a strain of *Euplotes* that he identified as *E. balteatus,* in which cells ranged in size from the normally occurring 30–50 μm morph to 120–200 μm giants, depending on their diet. This hypothesis about the scaling of adoral membranelles could perhaps be tested using microsurgical techniques to remove certain membranelles and observe the effects on feeding.

As the function of the dorsal cilia is not known (they are immobile), we cannot speculate on selective constraints affecting either corticotype or kinetotype. Since the numbers of dorsal cilia and of adoral membranelles both scale with cell size, which formed a continuum among our strains, these features should not be used diagnostically, as they so often have been in the classical literature [6, 7, 11, 47]. For example, *E. quinquecarinatus* has been distinguished from *E. charon* is that "there are always 9 rows of cilia, compared with 12 in *E. charon*"; otherwise, in silverline system, it "is extremely similar to *E. charon,* both ventrally and dorsally" [6].

It has been shown, in this study and others [16, 17, 18, 19, 25, 29, 33–35], that many of the "diagnostic" morphological criteria in the *Euplotes* taxonomic literature (e.g. cell size, number of adoral membranelles, corticotype, macronuclear shape, and position of the central fibril in the double dargyrome) are too variable within strains to be used as distinctions among strains. In other words, they are taxonomically uninformative. The only morphological features that are stable enough to be diagnostic are: cirrotype, basic cirral pattern and dargyrome type. Therefore, species descriptions based on morphological features other than these may be questionable and should be regarded with skepticism.

There are non-morphological criteria which have been used in the diagnosis of *Euplotes* species, such as habitat and encystment capability [11, 39]. Habitat is usually only reported crudely as that salinity category (marine, brackish, freshwater) from which the strains were collected; despite occasional reports of euryhaline strains, only rarely have strains consistently been tested to see if they can thrive to another salinity category. Our strains Cal4 and Galv1 are euryhaline strains of the *charon* morphotype, but they are quite similar to the described "freshwater" species *E. crenosus* [11], *E. inkystans* [47], and especially *E. palustris,* which was reported to encyst [46]. Encystment was noted in classical descriptions of *E. charon* [11, 50]; it was observed in our strains Cal4, CC31, Jam6, Jfla5, KK8, and Kli2. The genetic loci involved in encystment are not known, so it is not clear whether the capability represents enough of a difference to be considered diagnostic for species distinctions within a single morphotype. Our encysting strains span the entire morphometric spectrum that was examined in this study.

We have demonstrated here that, within the *E. charon* morphotype, the numbers of adoral membranelles and of dorsal cilia correlate positively and significantly with cell size, as do measures of oral cavity length, width, and area. Furthermore, cell size ranges over a broad continuum across strains. The only break in this size continuum we observed was that between strain Kli2 and the others, which simply is due to the fact that the other strains used in this study were selected from those in our stock cultures that had been identified as *E. charon* morphotype and "small." Strain Kli2 was a "medium" strain that was included initially for comparison with strain Kli3, a "small" strain from a nearby locality. It is possible that if other "medium" strains are examined by the methods used in this study, then the continuum in cell size within the *charon* morphotype would be found to be more complete.

Nevertheless, the continuum among strains seen in this study encompasses several described marine species [see synopses in 6, 11, 47]: *E. alatus* Kahl, 1932; *E. antarcticus* Fenchel and Lee, 1972; *E. balteatus* Dujardin, 1841; *E. charon* Müller, 1786; *E. harpa* harpa Stein, 1859; *E. magnacirratus* Carter, 1972; *E. neapolitanus* Wichterman, 1964; *E. octocirratus* Agamaliev, 1967; *E. polycarinatus* Carter, 1972; *E. quinquecarinatus* Gelei, 1950; *E. rariseta* Carter, 1974; *E. trisulcatus* Kahl, 1932; and *E. tuffraui* Berger, 1965. The species of historical precedence in this morphotype is *E. charon* Müller, 1786.

At this point we could begin assigning, a posteriori, our strains to, and redescribing, existing species (which has been done several times over for many of the classic species, e.g. *E. charon* [2, 11, 47, 50] and *E. balteatus* [4, 11, 48]). For example, strain Del1, with an average length of 42.5 μm and width of 33.0 μm, with an average of 19.8 membranelles in the AZM, with 6–8 dorsal rows of cilia, and with an average of 5.9 cilia in the mid-dorsal rows, fits the classic description of *E. rariseta* [11, 12]. Similarly, *E. quinquecarinatus* [6, 28] could be represented by strain Kli2, with average dimensions of 77.1 by 55.3 μm, 38.5 AZM membranelles, 8–10 dorsal rows, and 13.9 cilia in mid-dorsal rows. We probably also could describe a few "new" species. For example, strain Stv2, with dimensions of 40.7 μm in length and 26.8 μm in width, with six dorsal kineties, but with averages of only 18.7 AZM membranelles and only 7.2 cilia in the mid-dorsal row, does not match any of the published descriptions of cirrotype 10, double dargyrome *Euplotes* species. The most similar species is *E. rariseta,* which was described as never having more than 6 mid-dorsal cilia and as having around 23 AZM membranelles [12].

We, however, do not think that such descriptions and redescriptions of species help to understand the evolutionary relationships within this morphotype; it would only confuse the taxonomy if we were to present additional classical redescriptions. Our view is that the species listed above are simply descriptions of strains of a general morphotype which, in isolation, may possess characteristics apparently different from other described strains, but that these differences fade into continua when viewed in context with other strains. For this reason, we combine the above listed species under the nomenclaturally superior *E. charon.* We emphasize that this is not a species in one classical sense, in that it does not necessarily represent a genetically distinct group of populations; but it is a morphological species, or morphospecies, representing a group of strains which are variations upon a consistent morphological theme. In fact, the only strains in this study that we can be fairly sure belong to the same biological species are the three sympatric strains SI1, SI2, and SI4, because they conjugated with each other (though true conjugation was not confirmed by the split pair method [43]).

We maintain that available morphometric evidence does not presently justify any taxonomic distinctions within this broad

continuum. Progress is unravelling the fine-scale phylogenetic history of these common, small (and therefore often overlooked), cirrotype 10, double dargyrome *Euplotes* populations widespread in nature must await the application of such refined molecular techniques as rDNA sequence analysis [37, 53] to a collection of strains sufficiently diverse to encompass the range of morphological and geographic diversity reported herein.

ACKNOWLEDGMENTS

We are grateful to the following people for collecting samples which yielded some of the strains used in this study: Balinda Baldock, Karim Berrada, Chris Caprette, Josie Gaspano, Michael Hubley, Janet Joy, Michele Klingbeil, Jani Lewis, Laurence Packer, Janiel Shields and David Trueman. We particularly would like to thank Chris Caprette for initially cloning some of the strains and for constructive criticism.

LITERATURE CITED

1. Agamaliev, F. G. 1967. Faune des ciliés mésopsammiques de la côte ouest de la mer Caspienne. *Cah. Biol. Mar.*, **8**:359–402.

2. Agamaliev, F. G. 1974. Ciliates of the solid surface overgrowth of the Caspian Sea. *Acta Protozool.*, **13**:53–83.

3. Becker, R. A. & Chambers, J. M. 1984. S: An Interactive Environment for Data Analysis and Graphics. Wadsworth Advanced Book Program, Belmont, California. Pp. 550.

4. Berger, J. 1965. The infraciliary morphology of *Euplotes tuffraui* n. sp., a commensal in strongylocentrotid echinoids, with comments on echinophilous populations of *Euplotes balteatus* (Dujardin) (Ciliata: Hypothrichida). *Protistologica*, **1**:17–31.

5. Borror, A. C. 1963. Morphology and ecology of the benthic ciliated protozoa of Alligator Harbor, Florida. *Arch. Protistenk.*, **106**:465–534.

6. Borror, A. C. 1968. Systematics of *Euplotes* (Ciliophora, Hypotrichida): toward union of the old and the new. *J. Protozool.*, **15**:802–808.

7. Carter, H. P. 1972. Infraciliature of eleven species of the genus *Euplotes*. *Trans. Amer. Microsc. Soc.*, **91**:466–492.

8. Chatton, É. & Lwoff, A. 1930. Imprégnation, par diffusion argentique, de l'infracilature des ciliés marins et d'eau douce, après fixation cytologique et sans dessiccation. *Compt. Rend. Séanc. Soc. Biol.*, **104**: 834–836.

9. Corliss, J. O. 1979. The Ciliated Protozoa. Characterization, Classification and Guide to the Literature, 2nd ed. Pergamon Press, Oxford, U.K. Pp. 455.

10. Curds, C. R. 1974. Descriptions of three species of *Euplotes* (Protozoa: Ciliatea). *Bull. Br. Mus. Nat. Hist. (Zool.)*, **27**:113–127.

11. Curds, C. R. 1975. A guide to the species of the genus *Euplotes* (Hypotrichida, Ciliatea). *Bull. Br. Mus. Nat. Hist. (Zool.)*, **28**:1–61.

12. Curds, C. R., West, B. J. & Dorahy, J. E. 1974. *Euplotes rariseta* sp. n. (Protozoa, Ciliatea), a new small marine hypotrich. *Bull. Br. Mus. Nat. Hist. (Zool.)*, **27**:95–102.

13. Fenchel, T. & Lee, C. C. 1972. Studies on ciliates associated with the sea ice from Antarctica. I. The nature of the fauna. *Arch. Protistenk.*, **114**:231–236.

14. Frankel, J. & Heckmann, K. 1968. A simplified Chatton-Lwoff silver impregnation procedure for use in experimental studies with ciliates. *Trans. Amer. Microsc. Soc.*, **87**:317–321.

15. Gates, M. A. 1977. Analysis of positional information applied to cirral patterns of the ciliate *Euplotes*. *Nature*, **266**:362–364.

16. Gates, M. A. 1978a. An essay on the principles of ciliate systematics. *Trans. Amer. Microsc. Soc.*, **97**:221–235.

17. Gates, M. A. 1978b. Cirral patterns of cirrotype 9 *Euplotes* (Hypotrichida, Ciliophora). *Protistologica*, **14**:125–132.

18. Gates, M. A. 1978c. Morphometric variation in the hypotrich ciliate genus *Euplotes*. *J. Protozool.*, **25**:338–350.

19. Gates, M. A. 1985. Suggestions for revision of the ciliate genus *Euplotes*. *Atti Soc. Tosc. Sci. Nat. Mem., Ser. B*, **92**:43–52.

20. Gates, M. A. 1988. Dorsal kinetosomal distributions in the ciliate genus *Euplotes*. *J. Protozool.*, **35**:506–510.

21. Gate, M. A. 1990. Morphological drift accompanying nascent population differentiation in the ciliate *Euplotes vannus*. *J. Protozool.*, **37**:78–86.

22. Gates, M. A. & Berger, J. 1974. A biometric study of three strains of *Tetrahymena pyriformis* (Ciliatea: Hymenastomatida). *Can. J. Zool.*, **52**:1167–1183.

23. Gates, M. A. & Berger, J. 1976a. Morphological stability in *Tetrahymena pyriformis*. *Trans. Amer. Microsc. Soc.*, **95**:11–22.

24. Gates, M. A. & Berger, J. 1976b. Morphological inseparability of *Paramecium primaurelia* and *Paramecium pentaurelia*. *Trans. Amer. Microsc. Soc.*, **35**:127–134.

25. Gates, M. A. & Curds, C. R. 1979. The dargyrome of the genus *Euplotes* (Hypotrichida, Ciliophora). *Bull. Br. Mus. Nat. Hist. (Zool.)*, **35**:127–134.

26. Gates, M. A. & Ramphal, C. 1991. Daily rhythm of mating in the ciliated protist *Euplotes vannus*. *Trans. Amer. Microsc. Soc.*, **110**: 128–143.

27. Gates, M. A., Powelson, E. E. & Berger, J. 1975. Syngenic ascertainment in *Paramecium aurelia*. *Syst. Zool.*, **35**:127–134.

28. Gelei, J. 1950. Uj Euplotesek a tisza Vizrenszerebol. *Ann. Biol. Univ. Szeged.*, **1**:241–247.

29. Génermont, J., Machelon, V. & Demar, C. 1985. The "*vannus*" group of genus *Euplotes*. Sibling species and related forms: evolutionary significance and taxonomical implications. *Atti Soc. Tosc. Sci. Nat. Mem., Ser. B*, **92**:53–65.

30. Gianni, A. & Piras, L. 1993. Species structure in *Euplotes crassus* (Ciliophora, Hypotrichida). *J. Euk. Microbiol.*, **40**:155–161.

31. Jones, T. C. & Gates, M. A. 1994. A morphometric study of euryhalinity in marine populations of the ciliate genus *Euplotes*. *J. Euk. Microbiol.*, **41**:291–304.

32. Kahl, A. 1932. Urtiere oder Protozoa. I. Wimpertiere oder Ciliata (Infusoria), eine Bearbeitung der freilebenden und ectocommensalen Infusorien der Erde, unter Ausschluss der marinen Tintinnidae. *In*: Dahl, F. (ed.), *Die Tierwelt Deutschlands., Teil 25*. G. Fischer, Jena, Germany. Pp. 399–650.

33. Machelon, V. 1978. Etude d'une troisième espèce dans le complexe *Euplotes vannus* (Ciliés Hypotriches). *Protistologica*, **14**:15–22.

34. Machelon, V. 1982. Données sur le complexe *Euplotes vannus*: l'existence d'une cinquième espèce, analyse des mécanismes d'isolement reproductif. *Protistologica*, **18**:345–354.

35. Machelon, V., Génermont, J. & Dattee, Y. 1984. A biometrical analysis of morphological variation within a section of the genus *Euplotes* (Ciliata, Hypotrichida) with special reference to the *E. vannus* complex of sibling species. *Origins of Life*, **13**:249–267.

36. Morrison, D. F. 1967. Multivariate Statistical Methods. McGraw-Hill, New York. Pp. 338.

37. Olsen, G. J. 1988. Phylogenetic analysis using ribosomal RNA. *Meth. Enzymol.*, **164**:793–812.

38. Powelson, E. E., Gates, M. A. & Berger, J. 1975. A biometrical analysis of 22 stocks of four syngens of *Paramecium aurelia*. *Can. J. Zool.*, **53**:19–32.

39. Rawlinson, N. G. & Gates, M. A. 1986. A morphological classification of encysting species of *Euplotes* (Ciliophora: Nassophorea: Euplotida). *Trans. Amer. Microsc. Soc.*, **105**:301–310.

40. Sleigh, M. A. 1989. Protozoa and Other Protists. Edward Arnold, London, U.K. Pp. 342.

41. Small, E. B. & Lynn, D. H. 1985. Phylum Ciliophora Doflein, 1901. *In:* Lee, J. J., Hutner, S. H. & Bovee, E. C. (ed.), An Illustrated Guide to the Protozoa. Allen Press, Inc., Lawrence, Kansas. Pp. 393–408.

42. Sokal, R. R. & Rohlf, F. J. 1981. Biometry: The Principles and Practice of Statistics in Biological Research, 2nd ed. W. H. Freeman and Company, New York. Pp. 859.

43. Sonneborn, T. M. 1950. Methods in the general biology and genetics of *Paramecium aurelia*. *J. Exp. Zool.*, **113**:87–148.

44. Tatsuoka, M. M. 1971. Multivariate Analysis. John Wiley, New York. Pp. 310.

45. Taylor, W. D., Gates, M. A. & Berger, J. 1976. Morphological changes during the growth cycle of axenic and monoxenic *Tetrahymena pyriformis*. *Can. J. Zool.*, **54**:2011–2018.

46. Ten Hagen, R. 1980. Eine neue Susswasser-Euplotes-Art: *Euplotes palustris* n. sp. (Ciliophora, Hypotrichida). *Arch. Protistenk.*, **123**: 79–83.

47. Tuffrau, M. 1960. Révision du genre *Euplotes*, fondée sur la comparaison des structures superficielles. *Hydrobiologia*, **15**:1–77.
48. Tuffrau, M. 1964. Le maintien des caractères spécifiques à travers le polymorphisme d'*Euplotes balteatus* Dujardin, 1841. *Arch. Zool. Exp. Gén.*, **104**:143–151.
49. Tukey, J. W. 1977. Exploratory Data Analysis. Addison-Wesley Publishing Company, Reading, Massachusetts. Pp. 506.
50. Valbonesi, A., Ortenzi, C. & Luporini, P. 1987. Observations on the biology of *Euplotes charon* (Hypotrichida, Ciliophora). *Boll. Zool.*, **54**:111–118.
51. Valbonesi, A., Ortenzi, C. & Luporini, P. 1988. An integrated study of the species problem in the Euplotes *crassus-minuta-vannus* group. *J. Protozool.*, **39**:45–54.
52. Valbonesi, A., Ortenzi, C. & Luporini, P. 1992. The species problem in a ciliate with a high multiple mating type system, *Euplotes crassus*. *J. Protozool.*, **204**:171–180.
53. Van Keulen, H., Gutell, R. R., Gates, M. A., Campbell, S. R., Erlandsen, S. L., Jarroll, E. L., Kulda, J. & Meyer, E. A. 1993. Unique phylogenetic position of Diplomonadida based on the complete small ribosomal RNA sequence of *Giardia ardeae, G. muris, G. duodenalis* and *Hexamita* sp. *FASEB J.*, **7**:223–231.
54. Wichterman, E. 1964. Descriptions and life cycle of *Euplotes neapolitanus* sp. nov. (Protozoa, Ciliophora, Hypotrichida) from the Gulf of Naples. *Trans. Amer. Microsc. Soc.*, **83**:362–370.

Received 5-10-93, 2-11-94; accepted 3-7-94

J. Euk. Microbiol., 41(5), 1994, pp. 450–457

Napamichum cellatum N. Sp. (Microspora, Thelohaniidae), a New Parasite of Midge Larvae of the Genus *Endochironomus* (Diptera, Chironomidae) in Sweden

EVA K. C. BYLÉN[1] and J. I. RONNY LARSSON
Department of Zoology, Helgonav. 3, University of Lund, S-223 62 Lund, Sweden

ABSTRACT. The new microsporidium, *Napamichum cellatum*, a parasite of the adipose tissue of midge larva of the genus *Endochironomus* in Sweden, is described based on light microscopic and ultrastructural characteristics. Plurinucleate plasmodia with nuclei arranged as diplokarya divide, probably by plasmotomy, producing a small number of diplokaryotic merozoites. The number of merogonial cycles is unknown. Each diplokaryotic sporont yields eight monokaryotic sporoblasts in a thin-walled, more or less fusiform sporophorous vesicle. A small number of multisporoblastic sporophorous vesicles were observed, in which a part of the sporoblasts were anomalous. The sporogony probably begins with a meiotic division. The mature spores are slightly pyriform. Fixed and stained spores measure 2.1–2.4 × 3.7–4.5 μm. The five-layered spore wall is of the *Napamichum* type. The polar filament is anisofilar with seven to eight coils (142–156 and 120 nm wide). The angle of tilt is 55–65°. The polaroplast has an anterior lamellar and a posterior tubular part. The granular, tubular and crystal-like inclusions of the episporontal space disappear more or less completely when the spores mature. The crystal-like inclusions are prominent in haematoxylin staining, but not visible with the Giemsa technique. The microsporidium is compared to other octosporoblastic microsporidia of midge larva and to the species of the genera *Chapmanium* and *Napamichum*.

Supplementary key words. Taxonomy, ultrastructure.

IN the autumn of 1986, a microsporidium with lightly pyriform octospores was found in the adipose tissue of a midge larva collected in southern Sweden. The sporulation took place in lightly fusiform sporophorous vesicles with prominent crystalline inclusions. The parasite was tentatively identified as the species which, at that time, was known as *Chapmanium dispersus* Larsson, 1984 [5]. When the microsporidium was studied using electron microscopy several years later, it became apparent that it was a different species, one that belongs to the genus *Napamichum* Larsson, 1990 [6].

The microsporidium, which is new to science, is briefly described herein. It is compared to species of the genera *Chapmanium* and *Napamichum* and to octosporoblastic microsporidia from midge larvae. The taxonomic considerations are discussed with special attention to ultrastructural features.

MATERIALS AND METHODS

The host was one of two specimens of an unidentified species of the genus *Endochironomus* Kieffer in a sample of midge larvae collected from a pond at Vikhög in the region of Scania, southern Sweden, on October 7, 1986. To our knowledge it is impossible to identify midge larvae to species without rearing to adult stage, and that was impossible in this case.

Permanent squash preparations were lightly air dried, fixed in Bouin-Duboscq-Brasil solution overnight (Picric acid from Merck, Darmstadt, FRG) and stained using Giemsa (Fluka AG, Buchs, FRG) solution or Heidenhain's iron haematoxylin (Merck).

For paraffin sectioning, a few segments of the body were fixed in the same fixative overnight, washed and dehydrated in an ascending series of ethanols, cleared in butanol and embedded in paraplast. Sections were cut sagittally at 10 μm and stained using Heidenhain's iron haematoxylin. For details on the histological techniques, see the manual by Romeis [8]. All permanent preparations were mounted in DePeX (BDH Chemicals Ltd., England). Measurements were made with an eye-piece micrometer at ×1,000.

For transmission electron microscopy, one piece of an infected segment was excised and fixed in 2.5% (v/v) glutaraldehyde (BDH Chemicals) in 0.2 M sodium cacodylate buffer (pH 7.2) at 4° C for 4 h. After washing in cacodylate buffer and postfixation in 2.0% (w/v) osmium tetroxide (Agar Scientific Ltd., UK) in cacodylate buffer for 1 h in 4° C, the piece was washed and dehydrated in an ascending series of buffer-acetone solutions, to absolute acetone, and embedded in Epon. Sections were stained using uranyl acetate and lead citrate [7].

[1] To whom correspondence should be addressed.